International Journal of Bifurcation and Chaos

Structures out of Chaos in barred-spiral galaxies

P.A. Patsis
Research Center for Astronomy, Academy of Athens, Soranou Efessiou 4, GR-11527, Athens, Greece
patsis@academyofathens.gr

Received (to be inserted by publisher)

We review the dynamical mechanisms we have found to support morphological features in barred-spiral galaxies based on chaotic motions of stars in their gravitational fields. These morphological features are the spiral arms, that emerge out of the ends of the bar, but also the shape of the bar itself. The potentials used have been estimated directly from near-infrared images of barred-spiral galaxies. In this paper we present results from the study of the dynamics of the potentials of the galaxies NGC 4314, NGC 1300 and NGC 3359. The main unknown parameter in our models is the pattern speed of the system Ω_p. By varying Ω_p we have investigated several cases trying to match the results of our modeling with available photometrical and kinematical data. We found realistic models with stars on spirals in chaotic motion, while their bars are built by stars usually on regular orbits. However, we encountered also cases, where a major part of trajectories of the stars even in the bar are chaotic as well. Finally, we have examined the gas dynamics of barred-spiral systems, and we have found that the presence of gas reinforces the intensity of the "chaotic" spiral arms.

Keywords: Galaxies: kinematics and dynamics, Hamiltonian Systems, Response models

1. Introduction

Barred-spiral galaxies constitute one of the two types of disk galaxies, that are characterized by the presence of spiral arms. They possess, by definition, a central part elongated along an axis (the bar) and spiral arms, that have their roots at, or close to, the ends of the bar.

Statistics based on observations of large samples of disk galaxies in optical wavelengths have indicated that 25-35% are of SB type, i.e. they have strong bars [Sellwood & Wilkinson 1993]. Another 26% have a less conspicuous bar component and are classified as SBA, following the classification scheme in the "RC2" catalogue [de Vaucouleurs et al. 1976]. However, after the development of the near-infrared detectors in the '90s, it became clear that the morphology of the old stellar population, which is the important one for dynamical studies, is decoupled from the morphology in optical wavelengths, where young objects dominate. Bars, not observed earlier, have been discovered in the near-infrared in the central parts of the disks (see e.g. Grosbøl & Patsis [1998], and references therein). Eskridge et al. [2000] found that in the H-band ($1.65\mu m$), 56% of their sample is strong barred and another 16% weakly barred. Nowadays, there is a general agreement that most spiral galaxies are barred. Recent observations with the Spitzer Space Telescope have revealed, that also our Milky Way is a grand design barred-spiral galaxy [Churchwell et al. , 2009].

Nevertheless, not only near-infrared, but optical observations as well, are important for understanding the dynamics of bars. In these wavelengths another typical major morphological feature is observed, the dust lanes. The shape of these dust lanes has to be compatible with the overall dynamics dictated by the stellar bars. In the models, the morphologies foreseen for the observations of the galaxy at different wavelengths must be in agreement.

The understanding of the dynamics of barred-spiral galaxies is of crucial importance both for galactic as well as for extragalactic astronomy. On galactic scale, the dynamics of stars and gas is closely connected with star formation, since it determines the large scale distribution of the birth places of the stars on the disks. Even more important is the fact, that bars introduce in the system essentially a catalyst that controls secular evolution, i.e. morphological evolution within a Hubble time. They provide the mechanism for gas-inflow towards the centers of the galaxies, fuel star formation in their central parts, build boxy bulges, and feed black holes [see e.g. Kormendy & Kennicutt , 2004, and references therein]. Only by knowing the details of the dynamical mechanisms associated with these phenomena we will be able to fully understand secular evolution.

The dynamics of the bars provides information to, and simultaneously gets feedback from, disk galaxy formation scenaria. It is characteristic, that the fraction of barred-spirals declines strongly with redshift. At redshift z≈ 0.84 it drops to about 20%. However, this fraction refers mainly to the low-mass galaxies. Among the most massive galaxies, the fraction of bars is the same in the past as it is today [Sheth et al. , 2008]. This strongly indicates, that different initial conditions during the formation of galactic disks may lead to barred or non-barred spiral galaxies. We have also to have in mind, that post formation mergers may also have played a role in the today observed morphology of a galaxy. Finally, already early *N*-body simulations have shown [Hohl , 1971; Miller & Smith , 1979], that rotating bars are formed in disks very easily. However, the advancement of the modeling techniques and the increase of computing power has revealed that bars found in *N*-body models do not share the same properties. Especially the inclusion of the galactic bulges and the halos in self-gravitating form, introduced new phenomena in the simulations, like dynamical friction [see Sellwood , 2008, and references therein], and differentiated the properties of the *N*-body bars. The relation of all these models with the observed photometry and kinematics of real barred-spiral galaxies is currently an interesting open question in Galactic Dynamics.

Bars and spirals are density waves rotating in the disks, having their density maxima along an axis or along spiral arms, respectively. There is strong theoretical and observational evidence for this assumption [see e.g. Lin et al. , 1969; Rohlfs , 1977; Visser , 1980a,b; Grosbøl , 1994; Bertin , 2000]. Stars rotate with different angular velocities around the centers of the galaxies. There is only a characteristic distance from the center, where the stars and the waves rotate with the same frequency. This is the so called “corotation” resonance. In all rotating disk galaxies, there is a very important corotation zone, where the measure of the velocities of the stars is minimized or vanishes in the co-rotating with the bar (or the spiral) frame of reference.

An important remark in the research of the dynamics of galactic bars was made by Contopoulos [1980], namely that the x_1 family of periodic orbits is the main orbital backbone of the bars. The x_1 family is stable over long intervals of the Jacobi constant (E_J) and traps around it a large number of quasiperiodic orbits. It builds the bar, since the shape of its members is elliptical with apocentra roughly aligned along an axis. On the other hand, in the case of non-barred galaxies one can visualize the spiral waves by drawing ellipses precessing at a given rate [Kalnajs , 1973]. Contopoulos [1980], provided also evidence, that due to the topology of the x_1 orbits, bars cannot exceed in length the corotation distance. The role of the x_1 family and the corotation limit for the length of the bar still summarize the state of the art of our knowledge about the dynamics of galactic bars.

When the spirals beyond the ends of the bars are also considered, the dynamics become more complicated. Since the first attempts to understand the dynamics of these systems [Lindblad , 1947] it has been proven quite difficult to combine the dynamics of both components in a unique picture. A particular model was made by Sellwood & Sparke [1988], who found, that in their *N*-body models spirals and bars do not share the same pattern speed. This does not necessarily imply discontinuities in the barred-spiral structure.

Galactic images in the near-infrared, indicate, that in most barred-spiral systems the spirals are connected to the bar and emerge out of its end. This simple observation introduces a basic difficulty that has to be surpassed, namely the continuation of the spirals beyond the ends of the bar, through the corotation region, without any discontinuity. In the corotation region chaos dominates [Contopoulos & Grosbøl , 1989] and this has to be taken into account in models with a single pattern speed. Corotation in barred-spiral systems is close beyond the end of the bar, at distances where the strength of the m=2 component of the observed surface brightness is considerably strong if Fourier analyzed [see e.g. Aguerri et al. , 1998]. A first attempt to model barred-spiral galaxies by means of the orbital theory by Kaufmann & Contopoulos [1996] underlined for the first time the necessity to invoke chaotic orbits for building the part of the spirals that is closest to the bar. Also the study by Patsis et al. [1997] has shown that the characteristic outer boxy isophotes of the nearly face-on bar of NGC 4314 are due to chaotic orbits. These were indications that structure could, under circumstances, survive in chaotic zones as the corotation region in galactic disks.

Recently the role of chaotic orbits in supporting the spiral structure at the corotation region of barred-spiral galaxies has been the subject of many papers [see Voglis & Stavropoulos , 2005; Patsis , 2006; Voglis et al. , 2006; Romero-Gómez et al. , 2006; Tsoutsis et al. , 2008; Athanassoula et al. , 2009; Tsoutsis et al. , 2009; Contopoulos , 2009; Patsis et al. , 2010a; Harsoula et al. , 2011, and references in these papers]. The papers by Voglis and Harsoula et al., analyze N-body models, while the rest refer to analytic potentials. There is now a general consensus that at least part of the spirals are reinforced by stars in chaotic motion[1]. We will refer to this kind of spirals as "chaotic" spirals. However, important details related with the strength of the spirals that are formed by means of the proposed mechanisms, the efficiency of these mechanisms in supporting the spiral pattern, the role of the gas and the assessment of proposed alternative dynamics based on chaotic orbits are still under discussion.

We present here orbital models, that describe successfully the dynamics mainly of two grand design barred-spiral galaxies, NGC 4314 and NGC 1300. We mention also some results from the study of the NGC 3359 potential. The gravitational fields for these models have been estimated directly from near-infrared observations of these galaxies. In Section 2 we describe the observational principles on which the estimation of the potentials are based, the modeling assumptions and our method. The dynamics of NGC 4314 and NGC 1300 are discussed in Sections 3 and 4 respectively. In Section 5 we mention some results from the hydrodynamics of these models. They refer to NGC 3359 specifically and to the the overall flow of the gas. Finally in Section 6 we discuss and enumerate our conclusions.

2. Models for barred-spiral galaxies

2.1. *The estimation of the gravitational potential*

Images of galaxies taken in near-infrared bands are suitable for comparison with stellar dynamical models, because they detect primarily light from cool giants and dwarfs. These stars constitute the major fraction of the bolometric luminosity of a galaxy, thus the images are less affected by population effects than images taken in visual wavelengths. Also near-infrared images, especially in the K-band (around $2.2\mu m$), suffer less by dust attenuation and depict much more accurately the intrinsic shapes of galaxies. In conclusion near-infrared images trace better the mass distribution of the galaxies than images from any other passband. In addition inside the optical radius of the 25 mag arcsec^{-2} isophote the visible matter dominates and practically accounts for the observed rotation curves. So, dark matter can be ignored to a first approximation.

For these reasons the first step towards estimating gravitational potentials for galaxies is to obtain deep surface photometry in near-infrared bands. There are only two unknown parameters that one has to treat as free. The mass-to-light ratio (M/L) variation on the disk and the thickness of the galaxy. The assumption of a constant (M/L) ratio is in most cases practically acceptable and usually is adopted for the calculations. Our models are two-dimensional. However, we have to take into account the three dimensional light distribution. For the thickness of the disk we use in the most of our applications (in this and other papers) a law for the vertical, z, dependence of the density, $\rho_z(z)$, based on observations of disk galaxies of similar galactic type proposed by van der Kruit [1988]. Then, $\rho \propto \rho_z(z) = \frac{1}{2h_z}\mathrm{sech}^{2/n}\left(\frac{nz}{2h_z}\right)$, where h_z is the vertical scaleheight and n is an index. Other similar laws have been used by other authors for the estimation of the potential of disk galaxies [see e.g. Quillen et al. , 1994]. For the potential of the disk component on the galactic plane a Fourier decomposition method is used, that allows us to express it as a sum of trigonometric terms. In usual polar coordinates (R, θ), it is of the general form:

$$\Phi(R,\theta) = \Phi_0(R) + \sum_{k}^{k_{max}} \left[\Phi_{kc}(R)\cos(k\theta) + \Phi_{ks}(R)\sin(k\theta)\right]. \quad (1)$$

The range of k values in the sum is taken according to the needs of the modeling of every particular galaxy. The amplitudes of the trigonometric terms will be discussed separately for each case. Additional potential terms for a bulge and a dark matter halo are included in the NGC 1300 case, for a more realistic representation of the galaxy.

[1] A review of the research of the main groups that work on the subject can be found in the volume of the conference "Chaos in Astronomy" organized by the Research Center for Astronomy of the Academy of Athens [Contopoulos & Patsis , 2009].

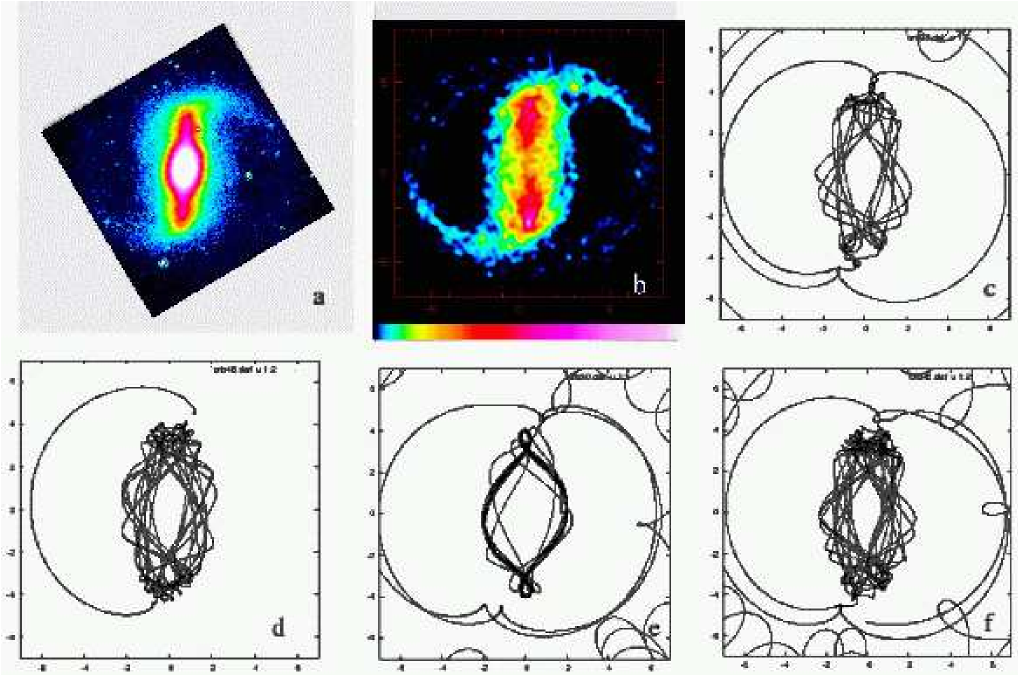

Fig. 1. (a) The DSS image of NGC 4314, (b) a response model that matches the main morphological features of the galaxy with Ω_p = 38.23 km s^{-1} kpc^{-1} . Density increases from the left to the right of the color bar at the bottom of the figure. (c to f) Chaotic orbits, which support the outer envelope of the bar and the spiral arms of the model.

2.2. *Modeling*

Our method is based on responses of, mainly, stellar disks, when we impose the estimated from the near-infrared observations galactic potential to a set of initial conditions. We work under the assumption, that, at least during the time we follow the response, the potential can be considered as time-independent, and that the bar and the spirals rotate with the same pattern speed. Equations of motion are derived from the Hamiltonian

$$H \equiv \frac{1}{2}\left(\dot{x}^2 + \dot{y}^2\right) + \Phi(x, y) - \frac{1}{2}\Omega_p^2(x^2 + y^2) = E_J, \tag{2}$$

where (x, y) are the coordinates in the Cartesian frame of reference, rotating with angular velocity Ω_p. $\Phi(x, y)$ is the potential in Cartesian coordinates. E_J is the numerical value of the Jacobi constant and dots denote time derivatives.

As regards the response models, we populate initially a disk within a R_{max} radius by placing 10^5 to 10^6 test particles at random positions and in circular motion in the axisymmetric part of the potential $\Phi_0(R)$. Since we deal with test particles and we study the dynamical mechanisms acting in different regions, there is no reason to populate exponentially the galactic disks. We grow the non-axisymmetric terms of the potential linearly from 0 to their final value within two pattern rotations. We integrate the particles' orbits for the time within which we want to follow the dynamical evolution of the system, that is for 10 pattern rotations. By continuing the integration of the orbits for more pattern rotations, we do not observe essentially any change in the morphology of the snapshots. Finally we construct density maps, by converting our data files to images using the ESO-MIDAS software. For this we consider a grid and we take into account the numerical density of the test particles on the disk.

3. NGC 4314

The first example we present here, refers to NGC 4314 an early type (SBa) barred spiral galaxy. The arms emerge out of the bar and the surface brightness along them decreases very fast as we deviate azimuthally away from the bar's ends. They fade out as we reach an angle about $\pi/2$. The galaxy is in a nearly face-on orientation in the sky and the main morphological features we discuss in this paper can be observed in the Digitized Sky Survey image we present in Fig. 1a. The surface brightness is given in logarithmic scale, that reveals also the boxiness of the bar in its outer parts. One has to observe the regions with yellow, especially green, and light blue pseudo-colors in Fig. 1a.

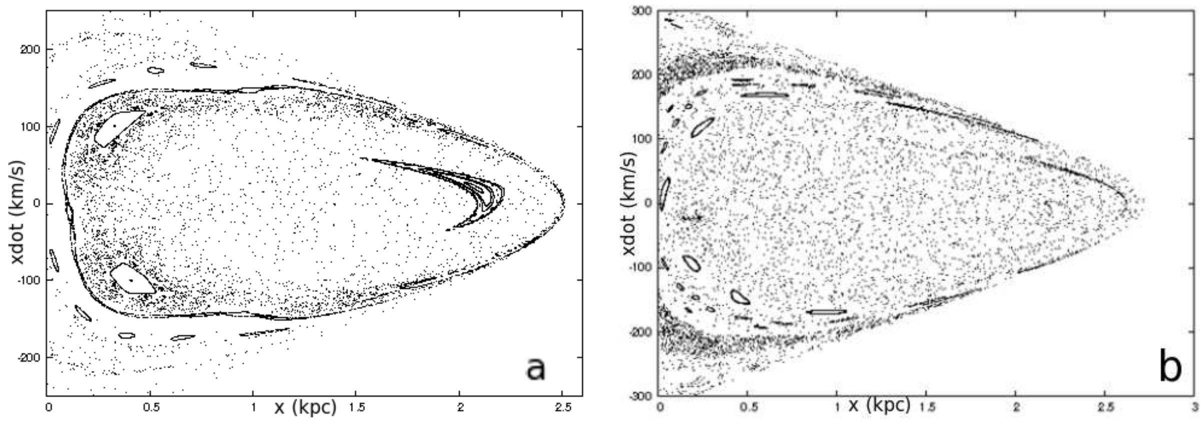

Fig. 2. $(x, \dot{x})$ surfaces of section that show the dominance of chaos in the E_J of the particles, that build the spiral arms of the model in Fig. 1b. In (a) for $E_J = -47500$ and in (b) for $E_J = -46000$. The cross sections are depicted for $0 < x < 2.6$ and $0 < x < 2.8$ respectively.

The light-blue region extends to larger radii and includes also the spiral arms. The boxiness of this bar is evident in the near-infrared images presented by Quillen et al. [1994], who have also estimated the potential in the plane of the galaxy based in these observations. They expressed it in the form of Eq. (1). In the particular case we have taken $k = 2, 4, 6$. The amplitudes of the components in Eq. (1) for the NGC 4314 potential are given in sums $\sum_n a_n r^n$ with coefficients α_n given in table 1 in Quillen et al. [1994], while for the vertical scale height we have adopted the value h_z=350 pc and the law of the vertical dependence of the density proposed by Quillen et al. [1994]. There is no explicit bulge component. However, this lack does not affect the dynamics in the outer parts of the bar.

Following the modeling procedure described in Sect. 2 we find that there is a good agreement between response models and the barred-spiral morphology of the galaxy for the range of pattern speeds 38.23< Ω_p <46 km s^{-1} kpc^{-1} . For these pattern speed values we have qualitatively the same dynamics that determine the morphology of the model and is in good agreement with the NGC 4314 structure. Patsis et al. [1997] have shown that the outer boxy shape of the bar is reinforced by particles in chaotic motion. The particular case studied in that paper was with Ω_p=44.96 km s^{-1} kpc^{-1} , but the same holds for all pattern speeds in the range the models succeed in matching the galaxy's morphology. Later Patsis [2006] has investigated in detail the orbital content for model (1) with Ω_p = 38.23 km s^{-1} kpc^{-1} and found that essentially the same trajectories that shape the outer envelope of the bar shape the spiral arms as well.

Following the methodology proposed by Patsis [2006] and used subsequently in other works studying structures emerging out of Chaos [Tsoutsis et al. , 2008; Chatzopoulos , 2010], we first isolate the particles found on the response model spirals and then we perform statistics of their Jacobi constants (E_J). In the case with Ω_p = 38.23 km s^{-1} kpc^{-1} we realize, that the vast majority of them are located in a narrow E_J interval $-48000 < E_J < -45000$ (km s^{-1})^2 [see figure 2 in Patsis , 2006]. The mode of the statistics is at $-48000 < E_J < -47500$ an interval that includes both the E_J of the unstable Lagrangian points L_1, L_2 and the E_J 's, where we find the rectangular 4:1 resonance family. The presence of this family indicates the location of the 4:1 resonance region in our model[2]. The tiny E_J interval in which the 4:1 family is stable, is just before the E_J of the unstable Lagrangian points. In these Jacobi constants chaos dominates on the $(x, \dot{x})$ surfaces of section. In Fig. 2 we give the surfaces of section for $E_J = -47500$ in (a) and $E_J = -46000$ in (b) for $0 < x < 2.6$ and $0 < x < 3$ respectively. One can easily find that the orbits of the particles on the spiral arms belong to the chaotic seas of the surfaces of section. Characteristic examples of the morphology of integrated initial conditions from the chaotic seas (for times corresponding to 10 pattern rotations) are given in Fig. 1 (c to f). All these chaotic orbits evidently reflect a strong 4:1 character in their morphology during a certain fraction of the integration's time. The spiral arms that are supported by them in the response model (Fig. 1b) match the arms of the galaxy (Fig. 1a). They emerge out of the bar and fade out at about a $\pi/2$ angle.

---

[2]The Hénon index α of the "rectangular" 4:1 resonance family is $-1 < \alpha < 1$ with a tangency at -1 in this tiny interval. In the same interval the Hénon index of the x_1 family levels off, which is a characteristic behavior of the index at the 4:1 resonance [Contopoulos & Grosbøl , 1989, see also figure 13 in Patsis et al. [1997]]

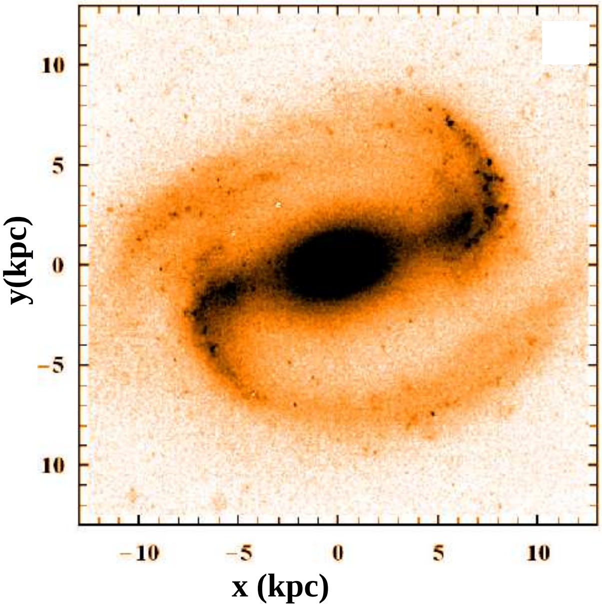

Fig. 3. A deprojected K-band image of NGC 1300 with (PA,IA)=(87°,35°)

4. NGC 1300 (in collaboration with C. Kalapotharakos and P. Grosbøl)

NGC 1300 is another grand-design barred-spiral galaxy of later type (SBbc). A deprojected K-band image of this galaxy is given in Fig. 3. From the dynamics point of view we focus on the shape of the bar that has two "blobs" at its ends, known as the "ansae", which differentiates it from the rectangular-like bar of NGC 4314. The arms are asymmetric, as well as the bar itself with respect to its center.

Starting from K-band observations with the SOFI instrument of the NTT telescope (ESO, La Silla), Kalapotharakos et al. [2010a] proposed three models that describe the potential of this galaxy. They differ in their geometry and allow for the inclusion of explicit bulge and dark matter components, i.e. $\Phi(R,\theta) = \Phi_{disk}(R,\theta) + \Phi_{bulge}(R) + \Phi_{halo}(R)$. The dark matter contribution has been estimated from published rotation curves [Lindblad et al. , 1997]. The disk component is again of the form given in Eq. (1). However, in order to study the observed morphological asymmetries, both even and odd terms are taken into account. We have $k = 1, \dots 6$. For the amplitudes of the trigonometric terms, a smoothed cubic interpolation scheme is used. The bulge and halo components are represented by Plummer spheres [Kalapotharakos et al. , 2010a]. Kalapotharakos et al. [2010b] have run a large number of response models by varying their pattern speeds in order to find the cases best reproducing the morphology observed in Fig. 3.

Patsis et al. [2010a] investigated the orbital dynamics of the models that matched at least partly the morphology of the galaxy. Here we present two of the cases that correspond to two different dynamical mechanisms leading to a realistic barred-spiral structure. In both of them all matter is considered lying on the galactic plane. This is a limiting case for the potential, which is called "Model A" in Kalapotharakos et al. [2010a]. It was realized that the main features of NGC 1300 were better reproduced in models clustered around two Ω_p values, namely 16 and 22 km s^{-1} kpc^{-1} . The effect of the variation of the pattern speed on the dynamics of the galaxy can be realized by observing the qualitative changes introduced in their effective potentials. This is shown in the two cases we describe below.

We underline, that our main goal here is to present dynamical mechanism we found to act in our models and result to a barred-spiral morphology and not to present a single best matching NGC 1300 model.

4.1. *Case 1*

The barred-spiral model in this case rotates with Ω_p=22 km s^{-1} kpc^{-1} . This leads to an effective potential with isocontours given in Fig. 4a. Compared with the original image of the galaxy the models are flipped in x and rotated

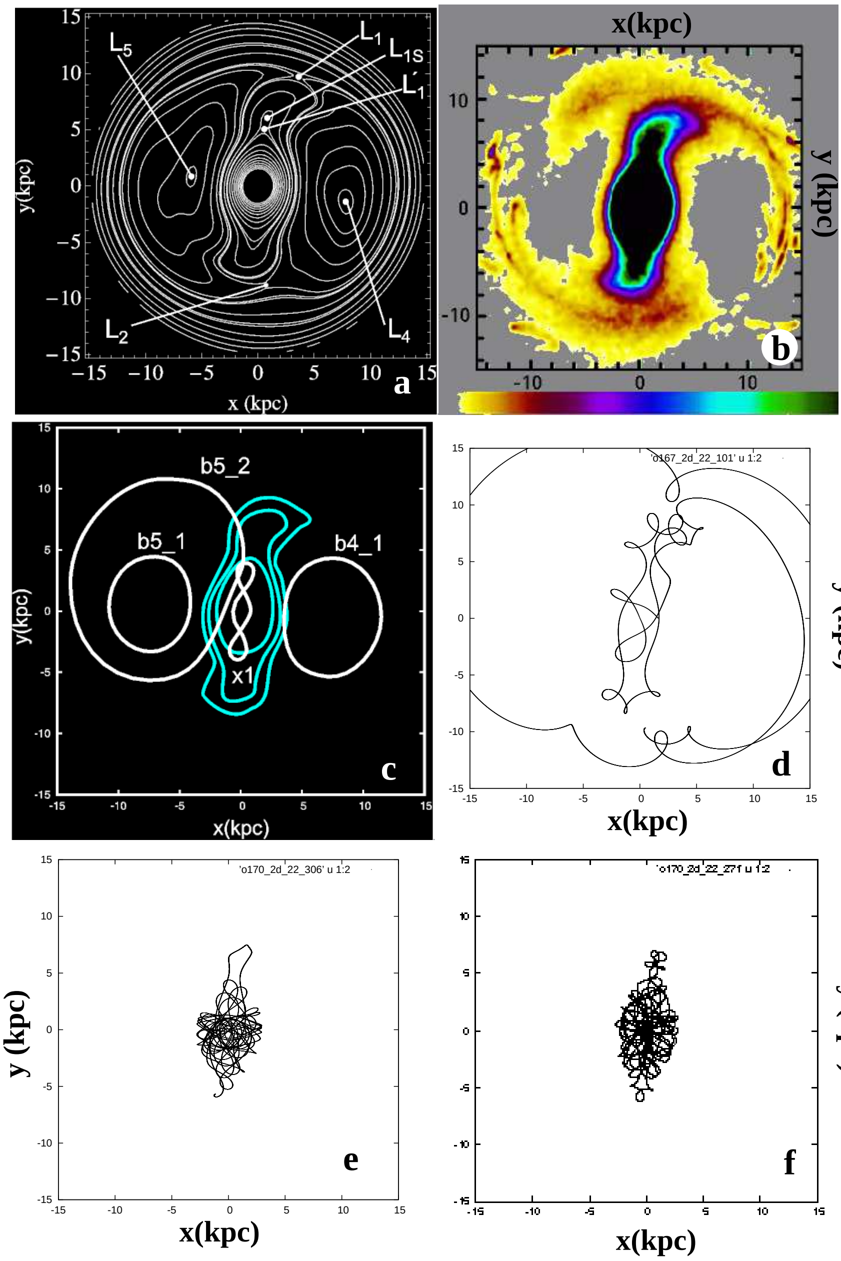

Fig. 4. **"Case 1"** model. (a) The effective potential. (b) The response model. Density increases from the left to the right of the color bar at the bottom of the figure. (c) The longest stable x_1 orbit and stable periodic orbits around L_4 and L_5 (white curves), together with isodensity contours of the model (light-blue curves). (d-f) Chaotic bar and spiral building orbits.

clockwise by $4\pi/9$ in order to facilitate the calculations, which are done by having the bar roughly along the y-axis and the system rotating counterclockwise. This holds for Fig. 4a and all subsequent figures referring to NGC 1300. The model is characterized by multiple stable and unstable Lagrangian points. Close to the major axis of the bar we have four Lagrangian points, three of which are unstable (L_1, L_1', L_2) and one stable L_{1S}. Fig. 4a describes the landscape of the effective potential. The particular shape of the isocontours has been proven to be decisive for the response models in all cases of the potentials for NGC 1300 we examined. For "Case 1" the isocontours form an ansae-type bar, more prominent in the upper part of the model ($y > 0$), due to the presence of the successive Lagrangian points close to the y-axis (L_1, L_{1S} and L_1'). The response model reflects this "ansae type" morphology of the bar (Fig. 4b). It has also two spiral arms beyond corotation. The orbital analysis by Patsis et al. [2010a] has shown

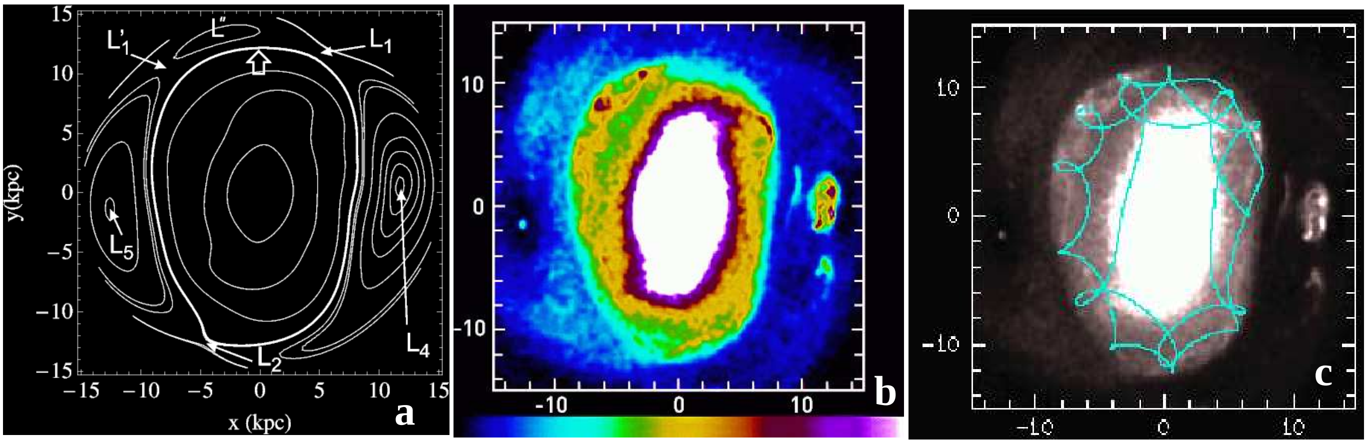

Fig. 5. **"Case 2"** model. (a) The effective potential. (b) The response model. Density increases from the left to the right of the color bar at the bottom of the figure.(c) Characteristic spiral building chaotic orbits. All axes are in kpc.

- first, that the spiral arms are formed through a mechanism involving the Lagrangian points L_1 and L_2 as in the NGC 4314 case and are composed by particles following chaotic orbits, and,
- second, that the majority of the particles building the bar are also in chaotic motion.

As regards the spirals, the particles on them belong to a hot orbital population [Pfenniger & Friedli 1991], that visits both the bar and the disk. This is similar to the NGC 4314 spirals, where most particles on them visit both the bar and the disk regions [Patsis , 2006]. Essentially, these are particles that spend time corresponding to several pattern rotations in the bar region and then diffuse to the disk. For the bar, in this particular model, the stable x_1 orbits can build only the central part of the bar by quasiperiodic orbits trapped around them. In Fig. 4c we have drawn the longest stable x_1 orbit we have found, together with stable orbits around L_4 and L_5 [Contopoulos & Grosbøl , 1989]. We also plot in Fig. 4c in light blue color characteristic isodensity curves of the model, that clearly show the small contribution of x_1 as well as of the families around the stable Lagrangian points in the response barred-spiral morphology. The rest of the structure is build by particles in chaotic orbits, as those given in Figs. 4d,e,f. They visit all allowed regions of the phase space at each Jacobi constant. The contraction and broadening of the isocontours in Fig. 4a allows for a similar "ansae type" morphology in the response bar. We note, that the orbits with Jacobi constants close to corotation, where we find the orbits that give to the bar its characteristic shape, contribute also to the surface density in the inner part of the bar, due to stickiness phenomena [Contopoulos & Harsoula , 2008] related with other families of periodic orbits existing for the same E_J 's.

4.2. *Case 2*

The only difference of this from the previous case, is that we have lowered the pattern speed from 22 km s^{-1} kpc^{-1} to Ω_p=16 km s^{-1} kpc^{-1} . Despite the fact that the corotation has moved a bit outwards, the length of the response bar is about the same as in Case 1. The spiral pattern reproduced by the response model consists of particles in chaotic orbits as well. However, the dynamical mechanism now is different from that of the previous case. As we can see in Fig. 5a the L_1 and L_2 points are away from the ends of the bar. The spiral arms that are formed in the response model (Fig. 5b) are now *inside* corotation. Due to the strong perturbation and the asymmetry of the model, we cannot draw a circle corresponding to a corotation circle in this model. The region inside corotation is separated from the region outside corotation by a more complicated curve. This is the thicker drawn isocontour of the effective potential in Fig. 5a, which is indicated with an arrow (upper part of the figure). The chaotic orbits of the particles on the spirals are in this case mainly of the kind we observe in Fig. 5c. This means, that the local density maxima on the spirals occur as the particles perform a motion like 'bouncing" on the heavy isocontour of Fig. 5a. In Fig. 5c a characteristic orbit has been plotted over a density map of the model, in which denser areas are colored with lighter shades. The perimeter of the grey region on which the orbit is "bouncing", practically coincides with the heavy isocontour of the effective potential in Fig. 5a. We have to note that the spiral arms formed with this mechanism in the model rotating with Ω_p=16 km s^{-1} kpc^{-1} we study here, represent best the spiral arms of NGC 1300. A detailed discussion about the model proposed as best matching the NGC 1300 morphology altogether can be found in Patsis et al. [2010a]. It is a combination of the model we propose in Case 2 for the spirals with a thick bar having cylindrical geometry and rotating with the same pattern speed. Here we have described the dynamical mechanisms that act in Cases 1 and 2 and result in very realistic morphologies.

5. NGC 3359 and gas models

5.1. *Hydrodynamics of NGC 3359*

Response models for the gas using potentials obtained from near-infrared observations have been studied with the method of Smoothed Particles Hydrodynamics (SPH) [Gingold & Monaghan , 1977; Lucy , 1977]. Assuming that the pattern speed in a galaxy is unique for the stellar and gas components, the dynamics of a gas model has to result to a morphology for the young objects on the disk compatible with the underlying stellar dynamics. The location of the young objects in the models has to be in agreement with what is observed in spiral galaxies [Grosbøl et al. , 2006]. Since the goal of the present paper is to review dynamical mechanisms that support realistic barred-spiral morphologies, we mention the recent paper by Patsis et al. [2009], where a model of the form given in Eq. (1) is used to study the dynamics of the late-type (SBc) barred-spiral galaxy NGC 3359. The amplitudes of the trigonometric components in this case are given in sums as in the NGC 4314 potential. This study has clearly shown, that the pattern speed of the *spirals* is such as to shift corotation close to the end of the spiral pattern. Then the loci of the HII regions on the galactic spiral arms are aligned along the response spirals, which are modeled with a "precessing ellipses" flow [figure 18 in Patsis et al. , 2009]. This flow has a backbone of stable precessing x_1 periodic orbits [figure 17 in Patsis et al. , 2009]. In order to combine this spiral with a bar of the size of the bar of the galaxy ending close to its corotation, one has to assume another, faster, pattern speed for the bar and accept a two pattern speeds system. In the proposed model the bar ends at its 4:1 resonance and the strong part of the spiral arms ends close to the 4:1 resonance of the slower rotating spiral pattern.

The model used for NGC 3359, for a range of Ω_p values, develops "chaotic" spirals according to the mechanism of Case 1 (Sect. 4.1). These spirals start close to the L_1 and L_2 points and the particles on them are in chaotic motion. However, these spiral arms do not match the spirals of NGC3359.

5.2. *Gas flow*

A detailed study of the gas response, in parallel with the stellar one, in potentials of the type of Eq. (1) is in progress by Patsis and Tsigaridi. Preliminary results have been presented in Tsigaridi & Patsis [2010]. Here we give a characteristic figure (Fig. 6), that summarizes the basic results. The potential is the one used by Patsis et al. [2009] for NGC 3359. However, now it is used for studying the general case of a barred-spiral system, without trying to reproduce the dynamics of the specific galaxy. In the case we present, the system rotates with Ω_p=30 km s^{-1} kpc^{-1} . The SPH model develops an inner bar with spirals emerging out of it, fading out very soon as they approach corotation (red circle in Fig. 6a). Beyond corotation, we observe another conspicuous bisymmetric spiral pattern. In Fig. 6b we give in enlargement the velocity vectors of randomly selected particles, plotted over the snapshot of the response model. The snapshot depicted in Fig. 6 is after 10 pattern rotations. The flow of the gas beyond corotation, and the streaming *along* the spirals, is similar with what we find for the stellar spirals, that originate close to the Lagrangian points L_1 and L_2 and are reinforced by chaotic orbits (as in Case 1 in Sect. 4.1). Despite their overall similarity, the streaming along the gaseous arms is larger than that along the stellar arms [Tsigaridi & Patsis , 2010]. As a result the relative amplitude of the m=2 component beyond corotation in the gas model is larger than that of the stellar one. This indicates that by means of this dynamical mechanism, in gaseous models, where we have small dispersions of velocities, are formed stronger spirals than in stellar models with large dispersion of velocities. This is in agreement with the result of Voglis et al. [2006], where strong "chaotic" spirals are formed in an *N*-body simulation, in which the dispersion of velocities of the stars in the initial conditions was taken to be small.

Finally, we mention the existence of dust lanes in the response of the gas in the bar of the potential of Case 1 (Sect. 4.1), which to a large extent, lacks the backbone of the x_1 family (Fig. 4c). This is especially interesting in the case in which a strong perturbation is introduced abruptly in the system. In that case the shape of the dust lanes can be like straight line segments [Patsis et al. , 2010b]. However in such a case we have a very strong inflow to the center of the galaxy.

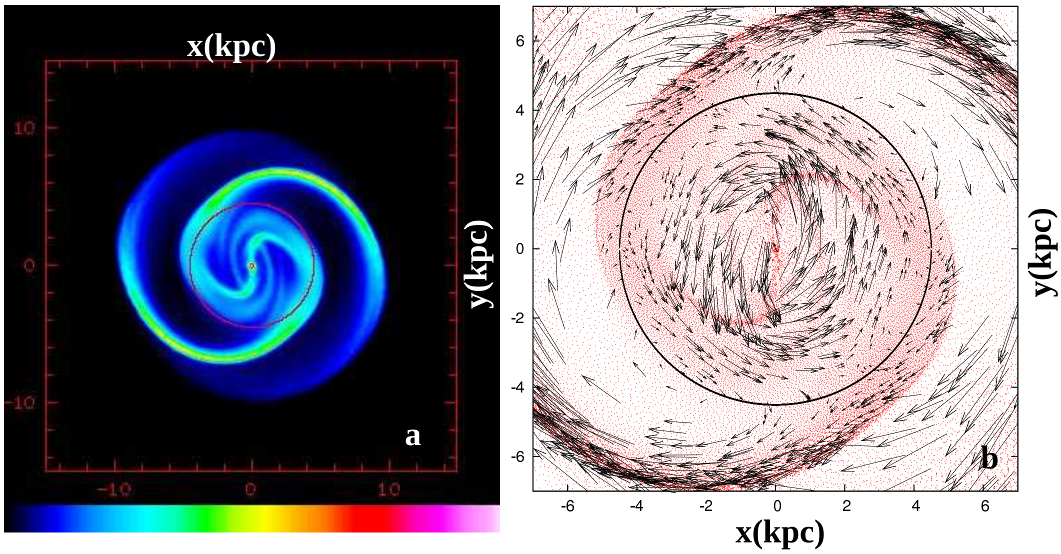

Fig. 6. An SPH model showing two types of flows. Inside corotation (drawn circles) we have a flow in agreement with the flow predicted by the families of stable periodic orbits of the stellar model. Outside corotation the flow is along the spirals, as in the case of the stellar "chaotic" spirals. In (a) we give the density map, and in (b) the velocity field. (a) and (b) frames are in different scales.

6. Summary and Conclusions

Response models based on potentials estimated from near-infrared observations have been proven to be a powerful tool for understanding the dynamics of barred-spiral galaxies. They introduce the least number of unknown parameters in the problem we study and for these parameters we can make plausible assumptions based on observations of samples of galaxies of the same type (e.g. for the thickness of the disk, the M/L ratio etc.). However, the main goal of this work is not to model the morphology of specific galaxies, but to test theories in models that reflect in some degree the complexity of real galaxies as dynamical systems. We do this by presenting some dynamical mechanisms that could have shaped the morphological features we observe. The results point to the dynamics of a class of galaxies with similar photometrical and kinematical properties. Due to the non-linear nature of the perturbations, the time needed for a feature (e.g. a bar) to obtain its shape is of the order of 1 Gyr, if we impose the potential to an axisymmetric background. Nevertheless, the models do not describe the morphological evolution of the disk during the lifetime of the galaxy.

In all these studies has been found a value of the pattern speed Ω_p, for which the response morphology matches a feature of the galaxy in detail. Our models suggest, that particles with E_J values close to corotation are very important, since they shape the morphology of the bar and may account also at least for part of the observed spirals. It is remarkable that we find these E_J values being populated by starting with initial conditions randomly distributed homogeneously on the disks in circular motion in the axisymmetric part of the potential (Φ_0 in Eq. 1). We introduce the full perturbation gradually over two pattern rotations.

Below we enumerate our main conclusions:

(1) Chaos plays a very important role in shaping barred-spiral galaxies, at least when the two components (bar and spiral) share the same pattern speed. For a coherent barred-spiral morphology with the bar ending close to corotation, this seems to be inevitable, since the structure has to survive in the chaotic zone of corotation. Kaufmann & Contopoulos [1996] have used chaotic orbits to bridge the region between the bar and the outer part of the spiral beyond the $-4:1$ resonance. However, recent studies suggest that in some cases the whole spiral structure, azimuthally extending more than an angle equal to π away of the bar's ends, may be composed by particles in chaotic motion [Voglis et al. , 2006; Romero-Gómez et al. , 2006; Tsoutsis et al. , 2008, 2009].
As regards the spirals of the models we discuss in the present paper, we have found that:

(a) In our models for early type *stellar* bars (Sect. 3) we have spiral arms beyond corotation supported by particles in chaotic orbits. They are formed by the mechanism involving unstable manifolds of unstable periodic orbits at E_J 's, where we find members of the unstable families around L_1 and L_2 as well as the 4:1 resonance family. The spiral supporting orbits in these E_J 's have morphologically a strong 4:1 resonance character in their parts inside corotation. The spirals formed this way fade out at an angle about $\pi/2$ away of the bar's ends.

(b) In models for later type bars (Sect. 4) we found also spirals supported by chaotic orbits, but *inside corotation*, via a dynamical mechanism summarized in Fig. 5 (Sect. 4.2). These spirals match the morphology of the spiral arms of NGC 1300. For a different Ω_p we find in the same models the "chaotic" spirals beyond corotation.

Our results for the bar component are the following:

(a) Besides the bars, which have as backbone the stable x_1 family in our models we find bars with their outer envelope made out of chaotic orbits. They have a rectangular-like shape as indicated by Patsis et al. [1997]. Chaotic envelopes of bars have been found also in bars in *N*-body simulations [Voglis et al. , 2006].

(b) We have found also a case with an ansae-type bar that is built essentially by chaotic orbits (Sect. 4.1). This model suggests a dynamical mechanism for building ansae-type bars by chaotic orbits. The mechanism is based on the presence of multiple Lagrangian points roughly along the major axis of the bar. Multiple Lagrangian points are necessary in order to build the appropriate shapes of the isocontours of the effective potential.

(2) Low dispersion of velocities in the initial conditions favor the formation of strong "chaotic" spirals beyond corotation. In gas response models the spirals beyond corotation are stronger than in the corresponding stellar models. In both of them the flow is *along* the arms.

(3) In the two pattern speeds case the corotation of the spiral pattern close to its end. There is a clear strong part of this spiral ending at its 4:1 resonance. The observed spiral morphology is compatible with a "precessing ellipses flow". Both bar and spirals are built by regular orbits. In this case we have a dynamical behavior similar to what we find in *normal* (non-barred) spiral galaxies.

Acknowledgments

I thank Prof. G. Contopoulos for fruitful discussions. This work has been partially supported by the Research Committee of the Academy of Athens through the project 200/739.

References

Aguerri J.A.L., Beckman J.E., Prieto M., 1998, AJ 116, 2136

Athanassoula E., Romero-Gómez M., Masdemont J. J. 2009, MNRAS 394, 67

Bertin G., 2000, '*'Dynamics of Galaxies"*, Cambridge Mas., CUP

Chatzopoulos S., 2010, *"Automatic Classification of Orbits in NGC 4314"*, Masters' Thesis, University of Athens, in Greek

Churchwell E., Babler B.L., Meade M.R. et al., 2009, PASP 121, 213

Contopoulos G., 1980, A&A 81, 198

Contopoulos G., 2004, *"Order and Chaos in Dynamical Astronomy"*, Springer-Verlag, New York

Contopoulos G., 2009, in "*Chaos in Astronomy*", G. Contopoulos and P.A. Patsis (eds), Springer-Verlag Berlin Heidelberg, pp. 3-22

Contopoulos G., Grosbøl P. 1989, Astron. Astroph. Rev. 1,261

Contopoulos G., Harsoula M., 2008, IJBC 2008, 18, 2929

Contopoulos G., Patsis P.A., 2009, "*Chaos in Astronomy*", Springer-Verlag Berlin Heidelberg

de Vaucouleurs G., de Vaucouleurs A., Corwin H.G., 1976, "Second Reference Catalogue of Bright Galaxies" (RC2), Univ. of Texas Press

Eskridge P.B., Frogel J.A., Pogge R.W. et al. 2000, AJ 119, 536

Gingold R.A., Monaghan J.J., 1977, MNRAS 181, 375

LNP 433, 101

Grosbøl P., Dottori H., Gredel R., 2006 A&A 453L, 25

Grosbøl P.J., Patsis P.A., 1998, A&A 336, 840
Harsoula M., Kalapotharakos C., Contopoulos G., 2011, MNRAS 411,1111
Hohl F., 1971, ApJ 168, 343
Kalapotharakos C., Patsis P.A., Grosbøl P. 2010a, MNRAS 403, 83
Kalapotharakos C., Patsis P.A., Grosbøl P. 2010b, MNRAS 408, 9
Kalnajs A.J., 1973, PASAu 2, 174
Kaufmann D.E., Contopoulos G., 1996, A&A, 309, 381
Kormendy J., Kennicutt R.C., Jr., 2004, Ann.Rev.A&A 42, 603
Lin C.C., Yuan C., Shu F. H., 1969, ApJ 156, 797
Lindblad B., 1947, PASP 59, 305
Lindblad P. A. B., Kristen H., Joersaeter S. and Hoegbom J., 1997, A&A 317, 36
Lucy L., 1977, AJ 82, 103
Miller R. H., Smith B. F. 1979, ApJ 227, 785
Patsis P.A., 2006, MNRAS 369L, 56
Patsis P. A., Athanassoula E., Quillen A. C., 1997, ApJ, 483, 731
Patsis P. A., Kaufmann D.E., Gottesman S.T., Boonyasayt V., 2009, MNRAS 394, 142
Patsis P. A., Kalapotharakos C., Grosbøl P., 2010a, MNRAS 408, 22
Patsis P. A., Kalapotharakos C., Grosbøl P., 2010b, MNRAS 409, L94
Pfenniger D., Friedli D., 1991, A&A 252, 75
Quillen A.C., Frogel J.A., Gonzalez R.A., 1994, ApJ, 437, 162
Rohlfs K., 1977, *"Lectures on Density Wave Theory (Lecture Notes in Physics)"*, Springer
Romero-Gómez M., Masdemont J. J., Athanassoula E., García-Gómez C. 2006, A&A 453, 39
Sellwood J.A., 2008, ApJ 679,379
Sellwood J.A., Sparke L.S. 1988, MNRAS 231, 25
Sellwood J.A., Wilkinson A., 1993, Rep.Prog.Phys. 56, 173
Sheth K., Elmegreen D.M., Elmegreen B.G. et al., 2008, ApJ 675, 1141
Tsigaridi L., Patsis P.A., 2010, in *"Advances in Hellenic Astronomy during the IYA09"*, ASP Conf. Ser. Vol. 424, K. Tsinganos, D. Hadzidimitriou, T. Matsakos (eds), pp.382-383
Tsoutsis P., Efthymiopoulos C., Voglis N., 2008, MNRAS 387, 1264
Tsoutsis P., Kalapotharakos C., Efthymiopoulos C., Contopoulos G., 2009, A&A 495, 743
van der Kruit P.C., 1988, A&A 192, 117
Visser H.C.D., 1980, A&A 88, 149
Visser H.C.D., 1980, A&A 88, 159
Voglis N., Stavropoulos I., 2005, in "*Recent advances in Astronomy and Astrophysics*", N. Solomos (ed), AIP Conference Proceedings, Volume 848, pp. 647-659
Voglis N., Stavropoulos I., Kalapotharakos C., 2006, MNRAS 372, 901